Finite Element Investigation of Optimal Reinforced Concrete Shear Wall Placement for Vibration Mitigation in Adjacent Buildings with Open-Trench Isolation

Mohammad Torabi Yazdi[a], Mohsen Farsiani[a,*]

[a] *Department of Civil Engineering, Sharif University of Technology, P.O. Box 11155-9313, Tehran, Iran*

Abstract

Vibration transmission in coupled soil–structure systems remains a fundamental challenge in the serviceability and resilience assessment of reinforced concrete (RC) buildings subjected to external dynamic excitations. Among the various sources of ground-borne vibration, railway-induced excitation constitutes a particularly significant engineering concern due to the continuing expansion of urban rail transportation networks and the increasing proximity of buildings to railway infrastructure. Motivated by this practical problem, the present study investigates the combined effectiveness of open-trench wave barriers and optimized shear wall placement for vibration mitigation in RC buildings subjected to railway-generated ground motion.

A two-dimensional plane-strain finite element framework was developed in ABAQUS to simulate the fully coupled soil–track–structure interaction problem. The computational model consists of a six-story RC frame structure founded on layered soil, a railway embankment subjected to dynamic excitation, and a 3 m-deep open trench positioned between the vibration source and the structure. To examine the influence of stiffness redistribution on structural vibration characteristics, four structural configurations were considered, including a reference model without a shear wall and three additional cases incorporating a 0.30 m-thick RC shear wall located in the first, second, and third structural spans, respectively. The numerical framework was verified

*Corresponding author

Email address: mohsen.farsiani95@sharif.edu (Mohsen Farsiani)

against established benchmark studies for ground-borne wave propagation and dynamic soil–structure interaction.

Structural vibration response was evaluated at multiple roof-level monitoring locations using peak particle velocity (PPV), root mean square velocity (RMS), and vibration decibel level (VdB). The results demonstrate that the open trench effectively attenuates incident wave energy before interaction with the structure, while the incorporation of strategically positioned shear walls further suppresses vibration transmission through enhanced global stiffness and altered dynamic load-transfer mechanisms. Among the investigated configurations, the shear wall located in the third span, corresponding to the span farthest from the excitation source, exhibited the highest mitigation efficiency, yielding reductions of up to 30.7% in PPV, 13.8% in RMS response, and 2.05% in VdB. The observed reductions indicate a substantial decrease in structural vibration demand and highlight the importance of stiffness distribution in controlling dynamic response characteristics.

The findings reveal a pronounced synergistic interaction between path-based isolation and receiver-based structural stiffening mechanisms and provide a mechanics-based framework for the vibration-resilient design and optimization of RC buildings subjected to externally induced ground vibrations.

Keywords: Train-induced vibration; Reinforced concrete buildings; Open trench barrier; Shear wall placement; Soil–structure interaction; Finite element modeling; Vibration mitigation

1. Introduction

Vibration propagation in coupled soil–structure systems has become an increasingly important topic in computational and applied mechanics due to its direct implications for structural serviceability, durability, and occupant comfort under dynamic loading environments. External vibration sources generated by transportation systems, industrial machinery, construction activities, and seismic disturbances can induce complex wave propagation phenomena within layered soil media and subsequently excite adjacent structures. Among these excitation sources, railway-generated ground vibration represents one of the most practically significant engineering problems because of the rapid global expansion of urban and high-speed rail transportation networks and the increasing proximity of railway infrastructure to densely populated urban regions. Although railway systems provide substantial environmental and economic advantages through sustainable transportation and reduced traffic congestion, the dynamic interaction between moving trains, track systems, and surrounding ground media can generate persistent vibration levels that adversely influence nearby buildings and sensitive facilities Kouroussis et al. (2014); Connolly et al. (2016); Zhai et al. (2019); Remennikov and Kaewunruen (2008). Excessive vibration amplitudes may negatively affect structural serviceability, human comfort, and the operational performance of vibration-sensitive infrastructures such as hospitals, laboratories, and heritage structures Adam and von Estorff (2005); Colaço et al. (2025); Jones and Block (1996); He et al. (2025). Furthermore, previous investigations have shown that layered and saturated soil conditions may substantially alter wave transmission characteristics, highlighting the necessity of accurately modelling realistic geotechnical environments in vibration analysis Li et al. (2019); Oner and Dong (1988).

Ground-borne vibrations generated by railway systems primarily originate from dynamic wheel–rail interaction mechanisms, including wheel and rail irregularities, axle impacts over sleepers, and coupled track–soil interaction effects. These dynamic excitations propagate through the ground predominantly in the form of Rayleigh surface waves and body waves, which may travel considerable distances with relatively low attenuation while inducing noticeable structural responses in adjacent buildings Zakeri et al. (2014). In urban environments characterized by heterogeneous layered soils and closely spaced infrastructure systems, the accurate characterization of wave propagation, scattering, and attenuation mechanisms becomes essential for reliable vibration prediction and mitigation. In addition, theoretical and numerical studies on wave propagation in layered elastic media have demonstrated that discontinuities, inclusions, and material heterogeneities can significantly influence wave scattering behavior and energy dissipation characteristics Peplow et al. (1999). Such observations further emphasize the importance of mechanics-based approaches for understanding vibration transmission in coupled soil–structure systems.

Existing vibration mitigation techniques are commonly categorized into source-based, path-based, and receiver-based strategies. Source-based approaches attempt to reduce vibration generation at the excitation source through modifications to the vehicle–track system, including resilient rail pads, ballast mats, and floating slab tracks. Receiver-based strategies focus on reducing the structural response through supplemental damping systems, base isolation, stiffness enhancement, and structural retrofitting techniques. In contrast, path-based mitigation methods aim to attenuate propagating waves within the transmission medium using trenches, buried barriers, or wave-impeding inclusions Buonsanti et al. (2009); Adam et al. (2000). Among these methods, open and in-filled trench systems have attracted considerable research attention because of their passive operational characteristics, practical implementation, and cost-effectiveness. Previous experimental and numerical investigations have demonstrated that open trenches and geofoam-filled barriers can effectively scatter and attenuate incident surface waves before they interact with nearby structures Beskos et al. (1986); Hung et al. (2004); Kontoni and Farghaly (2020); Zhao et al. (2025); Kattis et al. (1999); Leung et al. (1991). Nevertheless, the efficiency of trench-based isolation systems depends strongly on trench geometry, wave frequency content, and soil heterogeneity Kattis et al. (1999). Consequently, advanced computational approaches, including coupled finite element and boundary element formulations, have been widely employed to investigate transient wave propagation and evaluate vibration isolation performance under realistic soil conditions Mansur and Brebbia (1982).

In parallel with developments in path-based isolation systems, reinforced concrete (RC) shear walls have long been recognized as efficient structural components for improving the dynamic performance of buildings subjected to vibration and seismic loading. By increasing global lateral stiffness, modifying modal characteristics, and redistributing dynamic deformation demands, shear walls can substantially reduce structural vibration amplitudes under external excitations Jesmani et al. (2012). Furthermore, soil–structure interaction (SSI) effects may either amplify or attenuate the structural response depending on the relative stiffness and dynamic properties of the soil and superstructure Mylonakis (2000). Therefore, the distribution and placement of structural stiffening components within a building may significantly alter vibration transmission paths and overall dynamic behavior. Recent finite element investigations on coupled soil–track–structure interaction problems have further highlighted the importance of accurately representing structural stiffness distribution and SSI effects for reliable prediction of vibration response in adjacent buildings Grębowski and Zielińska (2026).

Recent advances in computational mechanics, wave propagation theory, and multiphysics modelling have considerably enhanced the capability of numerical methods to capture complex coupled-field interactions in engineering systems. Sophisticated mathematical frameworks developed for wave propagation in multiphase and multifunctional media have emphasized the importance of accurately characterizing material heterogeneity, coupled dynamic fields, and wave interaction mechanisms Shodja et al. (2023); Farsiani et al. (2024); Farsiani and Shodja (2026). Although such developments are primarily associated with advanced material systems, the underlying mechanics principles provide valuable insight into wave scattering, attenuation, and transmission phenomena governing vibration propagation in coupled soil–structure environments. These theoretical developments have consequently strengthened the role of high-fidelity finite element modelling in the analysis and mitigation of externally induced structural vibrations.

Despite the substantial body of literature devoted individually to trench-based isolation systems and structural stiffening techniques, their combined implementation for vibration mitigation in RC buildings remains insufficiently understood. In particular, limited attention has been given to the interaction between path-based wave attenuation mechanisms and in-structure stiffness redistribution achieved through optimized shear wall placement. Addressing this research gap, the present study investigates an integrated vibration mitigation strategy combining open-trench wave isolation with receiver-based structural stiffening. A two-dimensional plane-strain finite element framework is developed in ABAQUS to simulate the coupled soil–track–structure interaction problem for a six-story RC building adjacent to a railway line. Four structural configurations are examined, including a reference model without shear walls and three additional cases incorporating a 0.30 m-thick RC shear wall positioned respectively in the first, second, and third structural spans. Structural vibration response is evaluated using Peak Particle Velocity (PPV), Root Mean Square velocity (RMS), and vibration decibel level (VdB) measured at multiple roof-level monitoring locations. Through this parametric investigation, the study aims to identify the shear wall configuration that most effectively complements trench-based wave isolation and to provide a mechanics-informed framework for the design of vibration-resilient RC buildings subjected to externally induced dynamic excitations.

2. Modeling Framework

The present study develops a comprehensive finite element framework to investigate the effectiveness of integrated path-based and receiver-based mitigation strategies for reducing externally induced ground-borne vibrations in adjacent reinforced concrete (RC) buildings. Although railway-generated excitation is considered herein as a representative engineering application, the proposed framework is generally applicable to coupled soil–structure systems subjected to dynamic loading environments. Particular emphasis is placed on the role of reinforced concrete shear walls as structural stiffening components capable of modifying the global dynamic characteristics of the structure, including lateral stiffness, modal properties, dynamic load-transfer mechanisms, and vibration transmission paths. Through redistribution of structural stiffness and enhancement of overall frame rigidity, shear walls may substantially influence the propagation, amplification, and attenuation of vibration energy throughout the superstructure.

To accurately capture these coupled mechanisms, the modelling approach integrates the dynamic interaction among the excitation source, railway track system, surrounding soil medium, open-trench wave barrier, and multi-story building within a unified computational environment. The numerical framework is developed in ABAQUS using a two-dimensional plane-strain finite element formulation capable of representing transient wave propagation and coupled soil–track–structure interaction phenomena under dynamic excitation. The adopted formulation enables simultaneous simulation of wave generation, propagation through heterogeneous soil layers, interaction with the trench barrier, and subsequent transmission into the adjacent structure.

The computational domain consists of four principal components: the railway embankment and track system, the layered soil profile, the open-trench isolation barrier, and the six-story RC frame building. Railway-induced excitation is represented through a moving dynamic load applied at the rail level, thereby simulating the transfer of vibration energy generated by the train–track interaction into the supporting soil medium. The resulting wave propagation through the layered ground and its interaction with both the trench barrier and the adjacent structure are explicitly captured within the finite element model. Particular attention is devoted to accurately representing the coupled dynamic behavior of the soil and structural domains in order to evaluate the influence of shear wall placement on vibration attenuation characteristics and overall structural response.

To evaluate the influence of structural stiffness redistribution on vibration mitigation performance, several structural configurations are considered within the numerical framework. A reference configuration without shear walls is first analyzed to establish the baseline dynamic response of the building under externally induced ground excitation. Subsequently, three additional configurations are investigated by incorporating a 0.30 m-thick reinforced concrete shear wall within different structural spans of the building. This parametric arrangement enables a systematic assessment of the influence of shear wall placement on the transmission, redistribution, and attenuation of vibration energy within the superstructure. In the present study, railway-generated excitation is employed as a representative example of externally induced vibration loading in order to evaluate the effectiveness of the proposed mitigation strategy under realistic dynamic conditions.

The open trench is positioned between the railway track and the adjacent structure to function as a path-interruption barrier for incident surface waves propagating through the soil medium. The trench geometry and location are selected based on commonly adopted vibration isolation configurations reported in the literature. Particular attention is devoted to the interaction between the scattered wave field generated by the trench and the modified dynamic characteristics of the shear-wall-stiffened structure. This coupled interaction mechanism constitutes the central focus of the present investigation and provides insight into the synergistic behavior of path-based and receiver-based vibration mitigation approaches.

The structural response is evaluated using widely adopted vibration performance indicators, including Peak Particle Velocity (PPV), Root Mean Square velocity (RMS), and vibration decibel level (VdB). These response quantities are monitored at multiple roof-level locations in order to capture the spatial variation of structural vibrations and to quantitatively assess the effectiveness of each mitigation configuration. The proposed computational framework therefore provides a robust mechanics-based platform for investigating the coupled influence of wave-isolation barriers and structural stiffness enhancement on vibration mitigation in reinforced concrete buildings subjected to external dynamic excitations.

2.1. Geometric Configuration

The geometric configuration of the numerical model is illustrated in Figure 1. The railway embankment, representing the primary excitation zone, has a width of 6 m and a height of 1.5 m. Dynamic loads corresponding to train axle forces are applied as two parallel vertical line loads along the rail locations, symmetrically positioned to represent realistic loading conditions.

A rectangular open trench with a depth of 3 m and a width of 1 m is incorporated between the railway embankment and the adjacent building to attenuate the propagation of both surface (Rayleigh) waves and body waves through the supporting soil medium. The selected trench dimensions are consistent with established vibration isolation criteria reported in the literature, which indicate that open trenches become effective when their depth approaches at least one-half of the Rayleigh wavelength associated with the dominant excitation frequency, whereas rigid barriers such as concrete walls or steel piles are generally more efficient in soft soil conditions Sadeghi et al. (2025). The trench is positioned at a horizontal distance of 5 m from the embankment toe, yielding an overall separation of approximately 20 m between the railway track centerline and the building façade.

The soil domain is divided into two computational regions: a near-field finite-element zone and a far-field infinite-element zone. The near-field region explicitly captures wave scattering and soil–structure interaction effects, while the infinite-element region represents the unbounded soil medium and prevents artificial wave reflections at model boundaries.

The six-story reinforced concrete (RC) building is located 15 m behind the trench and has a width of 12 m and a total height of 18 m, corresponding to a story height of 3 m. Structural members (beams and columns) have cross-sectional dimensions of 0.6×0.3 m. When included, the shear wall has a uniform thickness of 0.3 m. The building is supported by a foundation slab with a thickness of 0.8 m, embedded 1.5 m into the subgrade.

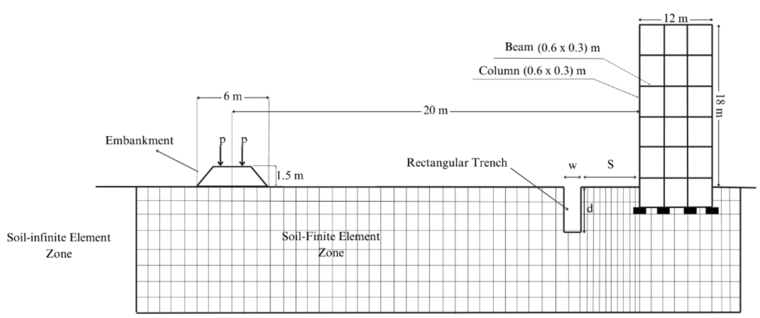

Figure 1: Model geometry showing embankment, trench, soil domain, and building layout

To investigate the influence of structural stiffness distribution on vibration mitigation, three shear wall configurations were considered: placement in the left bay (Span 1), central bay (Span 2), and right bay (Span 3). This parametric configuration enables direct evaluation of how the location of structural stiffening interacts with vibration attenuation produced by the trench barrier.

The overall model dimensions were selected based on established recommendations in the literature Beskos et al. (1986); Hung et al. (2004) to minimize boundary effects on wave propagation. Additionally, mesh refinement was applied in critical regions between the trench and the building to accurately capture wave scattering, diffraction, and mode conversion phenomena Adam and von Estorff (2005).

2.2. Material Properties

The mechanical properties assigned to the model components were selected based on previously validated studies on railway-induced ground vibrations and rail–soil–structure interaction Zakeri et al. (2014). The adopted parameters are summarized in Table. 1 and 2.

Material	Density ρ (t/m^3)	Poisson's ratio ν	Young's modulus E (MPa)
Subgrade soil	2.0	0.33	119.7
Embankment fill	2.0	0.33	332.5
RC foundation	2.5	0.20	34,560
Beams & columns	2.5	0.20	34,560
Shear wall (RC)	2.5	0.20	34,560

Table 1: Mechanical properties of soil and structural materials used in the finite element models

Material	Shear modulus G (MPa)	SWV (m/s)	CWV (m/s)
Subgrade soil	45	150	297.8
Embankment fill	125	250	496.3
RC foundation	14,400	2,400	3,919.2
Beams & columns	14,400	2,400	3,919.2
Shear wall (RC)	14,400	2,400	3,919.2

Table 2: Mechanical properties and associated elastic wave velocities of the soil and structural materials adopted in the finite element simulations. Here, SWV and CWV denote the shear wave velocity and compressional wave velocity, respectively.

In the numerical model, the embankment and subgrade soils are represented as linear elastic continua with small-strain material damping. This assumption is widely accepted for railway-induced vibrations, where the induced strain levels remain sufficiently small for soil behavior to remain close to its initial stiffness Mino et al. (2009). Under such conditions, nonlinear soil effects are limited, and the use of constant elastic moduli and damping ratios provides an adequate representation of the dynamic response.

Concrete structural components—including the foundation slab, beams, columns, and shear walls—are modeled as homogeneous linear elastic materials to capture their global stiffness characteristics. Although localized cracking and nonlinear behavior may occur under large loading conditions, these effects are negligible for the low-amplitude vibration levels considered in the present study. Therefore, a linear elastic representation is considered appropriate for evaluating the dynamic interaction between the soil, trench barrier, and structural system.

2.3. Boundary Conditions

To minimize spurious wave reflections at the model boundaries, absorbing boundary conditions were implemented along the lateral and bottom edges of the soil domain. This was achieved by combining infinite elements with viscous dashpot boundaries.

The infinite elements simulate a semi-infinite medium, allowing outward-propagating stress waves to exit the computational domain without artificial reflection. In ABAQUS, infinite elements are specifically formulated for this purpose to represent unbounded continua. In addition, viscous dashpots were applied at the boundaries to absorb residual wave energy and enhance attenuation over a range of incidence angles.

The dashpot damping coefficient is defined as

$$C_d = \rho V_s A, \tag{1}$$

where C_d is the dashpot coefficient, ρ is the soil density, V_s is the shear-wave velocity, and A is the associated boundary area. This expression is derived from the impedance of shear waves in an elastic medium and ensures that boundary energy dissipation is proportional to the dynamic characteristics of the soil.

The combined infinite-element and viscous-boundary approach has been widely adopted in ground vibration studies and has been shown to provide numerical stability while effectively suppressing artificial reflections Jesmani et al. (2012).

To ensure accurate simulation of wave propagation, the absorbing boundaries were positioned sufficiently far from both the excitation source and the structural domain. The overall model dimensions were selected based on the estimated Rayleigh wavelength, thereby minimizing boundary contamination of the primary wave field.

2.4. Loading Conditions

Train-induced excitation was modeled as a sequence of vertical rectangular pulse loads applied at the railhead locations (see Figure 2). Each pulse represents the passage of a single wheel axle moving at constant speed and is characterized by a peak line load of 1000 kN/m and a pulse duration of 0.02 s. The pulses are applied periodically with a repetition interval of $T = 0.02$ s, reflecting the regular spacing of axles along the train.

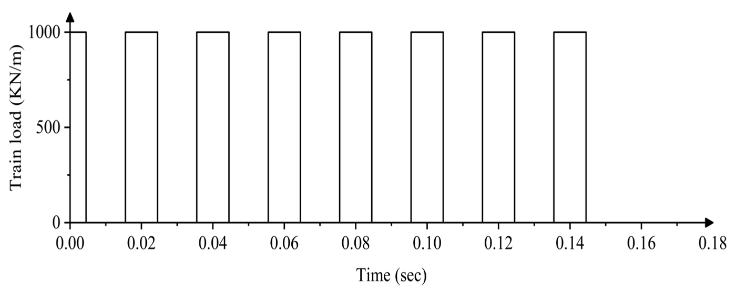

Figure 2: Time-history of the applied train pulse in the numerical model

This pulse-based loading formulation captures the transient and impulsive nature of railway excitation and is effective in exciting a broad frequency range of the coupled soil–structure system. Such an approach is well established in studies of train-induced ground vibrations and has been shown to adequately represent both near-field and far-field dynamic responses Jesmani et al. (2012).

In the numerical implementation, the excitation was applied as a distributed pressure along the rail cross-section. ABAQUS amplitude definitions were employed to prescribe the temporal evolution and duration of the loading pulses. To ensure consistency across all simulations, the load magnitude, duration, spatial distribution, and repetition interval were kept identical for all shear wall configurations, thereby isolating the influence of shear wall placement on the resulting vibration response.

2.5. Quantitative Vibration Metrics

To comprehensively evaluate the structural vibration response, three complementary indicators were adopted: Peak Particle Velocity (PPV), Root Mean Square velocity (RMS), and Vibration Decibel (VdB). These metrics jointly describe both the instantaneous and sustained dynamic characteristics of the structure under train-induced excitation. All parameters were computed from the vertical velocity time histories recorded at roof-level monitoring points A–D for the four structural configurations (No Wall, Span 1, Span 2, and Span 3).

Peak Particle Velocity (PPV). The peak particle velocity (PPV) represents the maximum absolute value of the vertical particle velocity during the observation period and is defined as

$$\mathrm{PPV} = \max_t |v(t)| \tag{2}$$

where $v(t)$ denotes the instantaneous vertical velocity. PPV characterizes the extreme response amplitude and provides a direct measure of transient excitation intensity. Elevated PPV values indicate pronounced dynamic impulses that may influence occupant comfort and induce localized structural stress concentrations, whereas reduced PPV values reflect effective attenuation of peak vibrations.

Root Mean Square Velocity (RMS). The root mean square (RMS) velocity quantifies the energy-equivalent vibration intensity sustained over a given time interval:

$$\mathrm{RMS} = \sqrt{\frac{1}{T_2 - T_1} \int_{T_1}^{T_2} v^2(t)\, dt} \tag{3}$$

where T_1 and T_2 denote the start and end times of the observation interval. RMS represents the average dynamic energy transmitted through the structure and is less sensitive to isolated transient peaks, thereby providing a stable and physically meaningful measure of overall vibration severity. Owing to these characteristics, RMS was adopted as the principal indicator for assessing vibration mitigation performance.

Vibration Decibel (VdB). The vibration decibel (VdB) expresses vibration magnitude on a logarithmic scale relative to a reference velocity, enabling interpretation in terms of human perception and serviceability:

$$\mathrm{VdB} = 20\log_{10}\left(\frac{V}{V_{\mathrm{ref}}}\right) \tag{4}$$

where V denotes the measured vibration velocity and the reference velocity is defined as $V_{\mathrm{ref}} = 0.0254 \times 10^{-6}\,\mathrm{m/s}$. In general, vibration levels below approximately 65 VdB are rarely perceptible to occupants, whereas levels exceeding 80–85 VdB may be perceived as disturbing. Consequently, this parameter provides a useful framework for interpreting the engineering results in terms of human comfort and building serviceability.

2.6. Analytical interpretation of the combined mitigation mechanism

Although the present study is conducted numerically, the observed response trends can be interpreted within a general dynamic framework for coupled soil–track–structure interaction. In the time domain, the governing equation of motion of the discretized system may be expressed as

$$\mathbf{M}\ddot{\mathbf{u}}(t) + \mathbf{C}\dot{\mathbf{u}}(t) + \mathbf{K}\mathbf{u}(t) = \mathbf{f}(t), \tag{5}$$

where $\mathbf{M}$, $\mathbf{C}$, and $\mathbf{K}$ denote the global mass, damping, and stiffness matrices, respectively, $\mathbf{u}(t)$ is the nodal displacement vector, and $\mathbf{f}(t)$ is the train-induced load vector. In the present problem, $\mathbf{f}(t)$ represents the transient axle loading transmitted through the rail and embankment into the supporting soil and, subsequently, into the adjacent building.

For harmonic components of excitation, Eq. (5) may be represented in the frequency domain as

$$\left(-\omega^2\mathbf{M} + i\omega\mathbf{C} + \mathbf{K}\right)\mathbf{U}(\omega) = \mathbf{F}(\omega), \tag{6}$$

where ω is the circular frequency, and $\mathbf{U}(\omega)$ and $\mathbf{F}(\omega)$ are the Fourier transforms of the response and load vectors, respectively. Equation (6) indicates that the vibration response depends not only on the excitation spectrum but also on the dynamic impedance of the coupled system. Accordingly, mitigation measures may act either by modifying the propagating wave field before it reaches the structure or by altering the structural receptance once the waves arrive at the foundation.

From this perspective, the open trench and the shear wall act through two complementary mechanisms. The trench primarily behaves as a wave-interruption barrier along the transmission path, reducing the amplitude of surface and near-surface waves propagating from the railway toward the building. By contrast, the shear wall modifies the internal stiffness distribution of the reinforced concrete frame, thereby changing its dynamic characteristics, including lateral stiffness, natural frequencies, and mode shapes. The combined system therefore constitutes a hybrid mitigation strategy in which the trench attenuates incoming motion in the soil, while the shear wall reduces the structural sensitivity to the residual vibration field.

To characterize this mechanism more explicitly, the response at a selected structural location j may be interpreted through a frequency-response function defined as

$$H_j(\omega) = \frac{U_j(\omega)}{F(\omega)}, \tag{7}$$

where $U_j(\omega)$ is the response spectrum at point j and $F(\omega)$ is the excitation spectrum. In practice, $H_j(\omega)$ represents the transfer characteristics of the coupled system from train loading to a structural response quantity of interest, such as displacement, velocity, or acceleration at the roof or upper-floor level. A reduction in the magnitude of $H_j(\omega)$ over the dominant excitation band implies improved vibration mitigation.

Based on Eq. (7), a frequency-dependent reduction factor may be introduced as

$$\eta_j(\omega) = 1 - \frac{|H_j^{\mathrm{mit}}(\omega)|}{|H_j^{\mathrm{base}}(\omega)|}, \tag{8}$$

where $H_j^{\mathrm{base}}(\omega)$ and $H_j^{\mathrm{mit}}(\omega)$ denote the transfer functions of the reference and mitigated configurations, respectively. Positive values of $\eta_j(\omega)$ indicate attenuation, whereas negative values would indicate amplification within a given frequency range. Although the present study evaluates mitigation primarily in the time domain through peak particle velocity (PPV) and root mean square (RMS) response, Eq. (8) provides a useful theoretical basis for interpreting why specific wall locations perform more effectively than others.

For practical comparison between configurations, the response reduction may be expressed in terms of a normalized time-domain index

$$\eta_r = \frac{R_{\mathrm{base}} - R_{\mathrm{mit}}}{R_{\mathrm{base}}} \times 100\%, \tag{9}$$

where R represents a scalar response metric such as PPV, RMS velocity, or vibration level at a selected monitoring point. This index is used in the present study to quantify the effectiveness of each shear wall arrangement relative to the corresponding baseline condition.

To generalize the interpretation of the numerical results, it is also useful to introduce several dimensionless parameters governing the mitigation problem. Let λ_R denote the Rayleigh wavelength associated with the dominant excitation frequency f_d, such that

$$\lambda_R = \frac{V_R}{f_d}, \tag{10}$$

where V_R is the Rayleigh wave velocity of the supporting soil. The relative effectiveness of the trench may then be related to the nondimensional trench depth and trench offset, respectively, as

$$\Pi_1 = \frac{D_t}{\lambda_R}, \qquad \Pi_2 = \frac{L_t}{\lambda_R}, \tag{11}$$

where D_t is the trench depth and L_t is the source-to-trench or trench-to-structure separation distance, depending on the adopted geometric reference. Similarly, the shear wall position may be represented by

$$\Pi_3 = \frac{x_w}{B}, \tag{12}$$

where x_w is the wall location measured along the plan width of the building and B is the total building width.

These dimensionless quantities are useful because they link the observed mitigation performance to fundamental wave-propagation and structural-layout characteristics rather than to a single case-specific geometry. In particular, the parameter Π_1 reflects the extent to which the trench depth is significant relative to the dominant wavelength of the incoming ground motion, while Π_3 describes the wall position relative to the building span arrangement. Within this framework, the superior performance of a wall placed in an intermediate span may be interpreted as the result of a more favorable redistribution of lateral stiffness and inertia, leading to lower structural receptance under the filtered vibration field transmitted beyond the trench.

Therefore, the effectiveness of the proposed mitigation system should not be viewed solely as the sum of two isolated measures. Rather, it arises from the interaction between path modification in the soil and stiffness reconfiguration in the structure. The trench alters the spectral content and amplitude of the incident motion reaching the building, whereas the shear wall governs how the modified excitation is transmitted and amplified within the frame. This interpretation provides a mechanistic basis for understanding the numerical findings and offers a more general framework for evaluating the optimal placement of shear walls in railway-adjacent reinforced concrete buildings equipped with open-trench isolation systems.

3. Results and Discussion

In this section, the generality and robustness of the proposed formulation are assessed through a series of representative examples encompassing diverse physical scenarios and varying levels of complexity. The first example is intended to verify the fidelity of the comprehensive soil–structure–railway interaction model. Specifically, the complete system—comprising the railway track, a 3 m-deep open trench, and a six-story reinforced-concrete (RC) frame without shear walls—is analyzed under the same geometric configuration and loading conditions previously reported in the literature. The problem is revisited here solely for verification purposes.

Subsequently, the robustness of the proposed framework is further demonstrated through additional examples of increased complexity, illustrating its applicability to a range of relevant problems.

3.1. Validation of the coupled soil–structure system

A comprehensive validation study was conducted to assess the accuracy and reliability of the proposed soil–structure–railway interaction model. The complete numerical system, comprising the railway track, a 3 m-deep open trench, and a six-story reinforced-concrete (RC) frame without shear walls, was analyzed under the same geometric configuration and loading conditions reported in Zakeri et al. (2014).

The validation was carried out based on the vertical velocity response at the roof level of the structure, which constitutes a critical measure of vibration transmission through the coupled soil–structure system. Figure. 3 compares the vertical velocity time histories obtained from the present ABAQUS simulation with the benchmark numerical results reported in Zakeri et al. (2014). An excellent agreement is observed between the two sets of results in terms of waveform evolution, peak occurrence, and overall attenuation behavior.

From a quantitative standpoint, the vertical velocity predicted by the present model ranges from -0.098 m/s to 0.027 m/s, which is in close agreement with the corresponding range reported in the reference study, namely -0.099 m/s to 0.020 m/s. The minor deviation observed in the positive peak response remains within the expected numerical tolerance and can reasonably be attributed to slight differences in mesh discretization, boundary-condition implementation, or time-integration parameters.

Overall, the comparison confirms that the adopted modeling framework, including the constitutive representation, damping formulation, and transient loading strategy, is capable of reproducing the dynamic response of the benchmark problem with a high degree of accuracy. The validated finite-element framework therefore provides a reliable basis for the subsequent parametric investigation of shear-wall configurations and trench–wall interaction effects in the mitigation of train-induced structural vibrations.

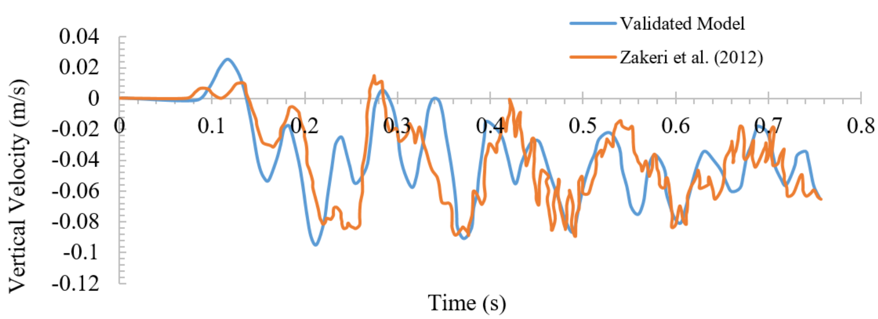

Figure 3: Validation of the coupled soil–structure interaction model based on the comparison of vertical velocity time histories.

3.2. Parametric modeling of shear wall placement

Building upon the validated finite element framework, a parametric investigation was conducted to evaluate the influence of shear wall location on the vertical vibration response of a six-story reinforced concrete (RC) building subjected to train-induced excitation. Four structural configurations were examined: a reference model without a shear wall and three alternative configurations in which a 0.3 m thick shear wall was installed in Span 1 (closest to the trench), Span 2 (mid-span), or Span 3 (farthest from the trench);Figure. 4.

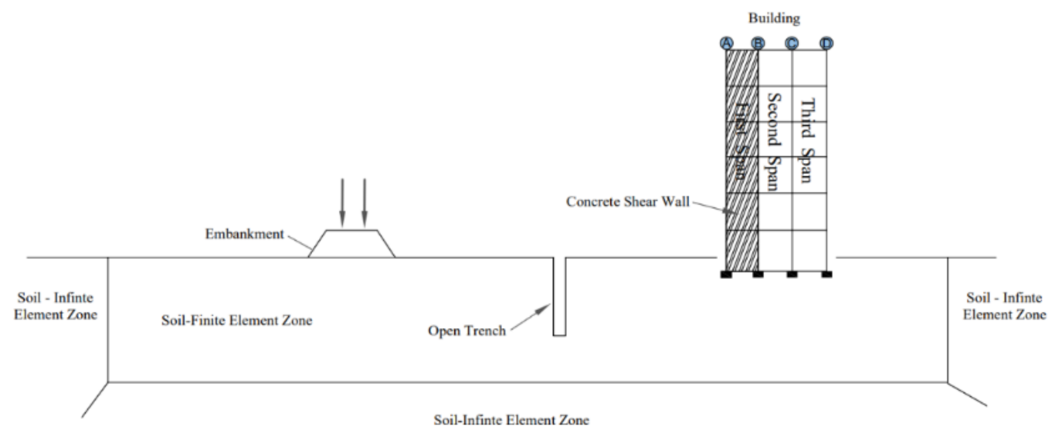

Figure 4: Schematic of the parametric model geometry and corresponding measurement locations considered in the shear wall placement study.

To isolate the influence of wall position, the shear wall was assigned the same material properties as the beams and columns of the RC frame ($E = 34{,}560$ MPa, $\nu = 0.20$, $\rho = 2.5$ t/m^3). All other modeling parameters, including soil stratification, trench geometry, and loading conditions, were maintained consistently across the investigated configurations. The open trench (3 m deep and 1 m wide) was positioned at a fixed offset of 5 m from the embankment toe and served as a passive vibration-isolation barrier. The applied excitation consisted of cyclic vertical loads of 1000 kN/m repeated at intervals of 0.02 s, representing the periodic axle loads generated by a passing train.

Vertical velocity time histories were recorded at four monitoring points (A–D) located at the roof level along the column lines. The corresponding responses for the different structural configurations are shown in Figure. 5. In the reference configuration without shear walls, the building exhibits relatively large vibration amplitudes accompanied by a gradual decay of oscillations, indicating limited structural damping and susceptibility to resonance effects.

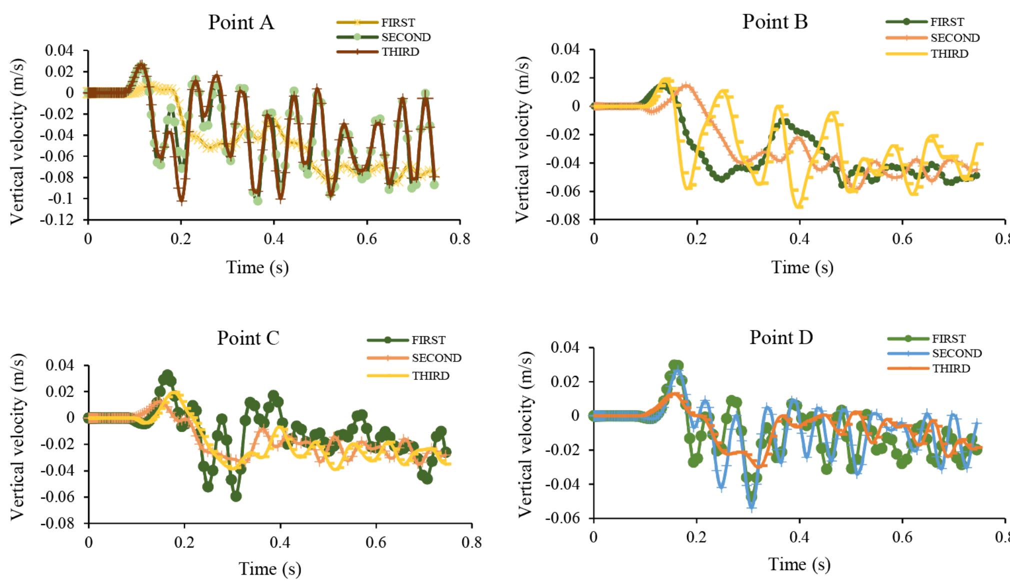

Figure 5: Vertical velocity time histories at roof-level measurement points A–D for different shear wall configurations (walls placed at Spans 1, 2, and 3, respectively)

Introducing a shear wall in Span 1 leads to a noticeable reduction in vibration amplitude near Point A, which is closest to the trench. However, slightly higher amplitudes are observed at the more distant monitoring points. This behavior suggests that the localized increase in stiffness may induce partial wave reflections within the structural system.

When the shear wall is placed in Span 2, the vibration response becomes more evenly distributed among the monitoring points. The corresponding time histories show smoother attenuation patterns and more comparable peak amplitudes across the roof level, although small residual oscillations remain.

The configuration with the shear wall located in Span 3 produces the most uniform response among all monitored points. In this case, the peak vertical velocities are consistently lower and the oscillations attenuate more rapidly compared with the other configurations. This behavior indicates that positioning the shear wall farther from the trench allows the structural system to redistribute vibrational energy more effectively.

From a physical perspective, this response can be interpreted as the result of a sequential mitigation mechanism between the trench and the shear wall. The open trench first scatters and attenuates a significant portion of the incoming surface waves before they reach the building foundation. The remaining vibrational energy is then further redistributed by the shear wall within the structural system. When the wall is located closer to the structural core (Span 3), the stiffness distribution becomes more balanced, reducing internal reflections and promoting smoother energy dissipation throughout the frame.

Overall, the numerical results indicate that increasing the distance between the trench and the shear wall tends to produce a more balanced vibration response across the structure. Among the investigated configurations, the Span 3 arrangement provides the most favorable performance in terms of reduced peak amplitudes and faster attenuation of oscillations. Consequently, this configuration is identified as the most effective wall placement for mitigating train-induced vibrations in RC buildings located adjacent to railway corridors.

3.2.1. Interpretation of Vibration Response Trends

Analysis of the vertical vibration responses reveals clear and consistent behavioral trends among the three investigated shear-wall configurations (Table. 3). When the shear wall was positioned adjacent to the trench (Span 1), both the Peak Particle Velocity (PPV) and the Root Mean Square (RMS) velocity measured at Point A, located directly above the wall, exhibited a pronounced reduction relative to the unbraced configuration. This behavior indicates significant near-field vibration attenuation and partial interception of the propagating wave energy.

Nevertheless, a slight increase in vibration amplitudes was observed at the far-side monitoring points (Points C and D). This phenomenon suggests that the abrupt stiffness discontinuity introduced at the wall–frame interface promoted partial internal wave reflections and a nonuniform redistribution of vibrational energy throughout the structural system.

Brace Location	Parameter	Vertical Velocity Position			
		A	**B**	**C**	**D**
First	PPV	0.0484	0.0454	0.0569	0.0329
	VdB	1.26	1.25	1.27	1.22
	RMS	0.0211	0.0179	0.0169	0.0129
Second	PPV	0.0690	0.0400	0.0330	0.0434
	VdB	1.29	1.24	1.22	1.25
	RMS	0.0263	0.0172	0.0132	0.0138
Third	PPV	0.0705	0.0404	0.0309	0.0282
	VdB	1.29	1.24	1.22	1.21
	RMS	0.0268	0.0169	0.0137	0.0110
No Brace	PPV	0.0721	0.0353	0.0446	0.0378
	VdB	1.29	1.23	1.25	1.23
	RMS	0.0275	0.0174	0.0153	0.0128

Table 3: Vertical vibration response parameters for different brace locations

Relocating the shear wall to Span 2 (mid-span) resulted in a more balanced dynamic response throughout the structural system. Both the Peak Particle Velocity (PPV) and Root Mean Square (RMS) velocity values exhibited moderate reductions at the intermediate monitoring points (Points B and C), indicating improved wave-energy diffusion and partial suppression of resonance phenomena. Nevertheless, minor oscillatory amplifications persisted near the free-edge region, suggesting that although the transmission of vibrational energy became more uniformly distributed, complete attenuation was not fully achieved.

The most uniform and globally effective vibration mitigation was observed for the Span 3 configuration, in which the shear wall was positioned farthest from the trench. In this case, all monitoring points (A–D) simultaneously exhibited reduced peak velocities, smoother oscillatory behavior, and faster attenuation rates. Moreover, the RMS values, which represent the cumulative vibration energy within the structure, decreased by nearly 50% relative to the unbraced configuration, demonstrating the superior damping efficiency of this arrangement together with its reduced susceptibility to resonance amplification.

The corresponding time-history responses for the Span 3 configuration also revealed more synchronized oscillation phases across the structural frame, confirming that the vibrational energy was absorbed and dissipated in a more coordinated and spatially uniform manner.

3.2.2. Normalization and Quantitative Comparative Assessment

To establish a consistent basis for comparison among the four investigated configurations—namely, the unbraced model (No Wall) and the three shear-wall arrangements (Span 1, Span 2, and Span 3)—all vibration-response parameters at monitoring points A–D were normalized with respect to the reference unbraced configuration. The normalization procedure expresses the relative percentage variation in vibration intensity, wherein negative values denote vibration reduction (mitigation), whereas positive values indicate amplification effects.

Table. 4 summarize the normalized values of the Peak Particle Velocity (PPV), Root Mean Square (RMS) velocity, and vibration decibel level (VdB), respectively. In addition, Figure. 6 illustrates the corresponding spatial distributions and comparative response trends for the investigated configurations.

Brace Location	**Parameter**	**A (%)**	**B (%)**	**C (%)**	**D (%)**
First	PPV	-32.8	28.4	27.4	-12.9
	VdB	-2.67	1.77	1.68	-0.97
	RMS	-23.3	2.67	10.0	0.79
Second	PPV	-4.27	13.3	-26.1	15.0
	VdB	-0.29	0.88	-2.10	0.98
	RMS	-4.47	-1.46	-14.1	8.40
Third	PPV	-2.11	14.5	-30.7	-25.3
	VdB	-0.14	0.96	-2.55	-2.05
	RMS	-2.69	-2.92	-10.6	-13.8

Table 4: Normalized vertical vibration response differences for different brace locations

The normalized comparisons provide clear insight into the relative effectiveness of the investigated shear-wall configurations. In terms of the Peak Particle Velocity (PPV), the Span 1 configuration produced a pronounced local reduction of approximately -33% at Point A; however, this improvement was accompanied by vibration amplification of nearly $+28\%$ at Points B and C. Such behavior indicates effective localized damping in the vicinity of the excitation source, but comparatively limited capability in achieving global vibration control across the structural system.

In contrast, the Span 3 configuration resulted in consistent PPV reductions of approximately -30% at Points C and D, demonstrating its superior ability to suppress peak vibration amplitudes throughout the structure in a more spatially uniform manner.

The Root Mean Square (RMS) responses, which represent energy-equivalent measures of vibration intensity, exhibited smoother and more physically interpretable trends. For the Span 1 and Span 2 configurations, the results remained mixed, with certain monitoring locations showing attenuation while others experienced slight amplification effects. By comparison, the Span 3 arrangement achieved RMS reductions at all monitoring points, with attenuation levels ranging from approximately -3% to -14%. This behavior further confirms the enhanced stability and uniform damping performance associated with the third-span configuration.

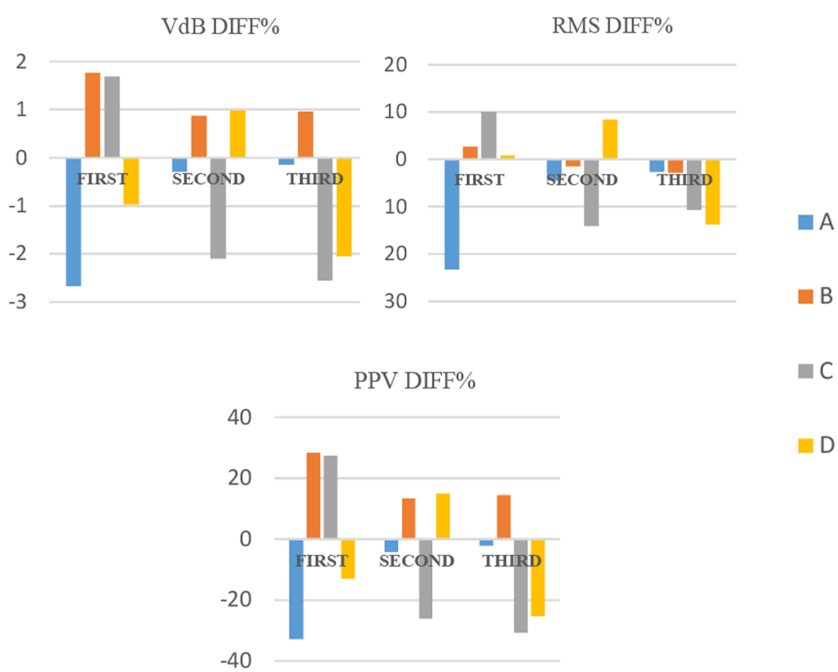

Figure 6: Comparative visualization of normalized vibration response differences, expressed in terms of peak particle velocity (PPV), vibration decibel level (VdB), and root mean square (RMS), at monitoring points A–D for the three shear wall configurations (Spans 1–3).

3.2.3. Mechanistic Interpretation: Trench–Wall Interaction

Due to its logarithmic definition, the vibration decibel parameter (VdB) exhibited relatively smaller variations, generally within ±3%. Nevertheless, the overall response trend remained fully consistent with the PPV and RMS observations, as only the Span 3 configuration produced uniform and perceptible reductions in the perceived vibration levels. These findings suggest improved structural serviceability and enhanced occupant comfort when the shear wall is positioned at the farthest location from the trench.

The vibration-response characteristics observed for the investigated configurations can be interpreted in terms of the coupled interaction between the open trench and the internal shear wall. The 3 m-deep trench functions as a primary wave barrier, scattering and reflecting a considerable portion of the incident Rayleigh and body waves before they reach the building foundation.

When the shear wall is positioned immediately behind the trench (Span 1), the residual high-energy waves interact with a stiff structural element at a short propagation distance. This abrupt impedance contrast promotes secondary wave reflections within the structural frame and may lead to localized amplification at remote regions of the structure.

By contrast, when the shear wall is located farther from the trench (Span 3), the trench first attenuates a substantial portion of the incoming vibration energy. The shear wall then acts as a secondary structural interface that redistributes and gradually dissipates the filtered wave energy throughout the building system.

This two-stage mitigation mechanism—consisting of initial wave interception by the trench followed by structural absorption and redistribution by the shear wall—explains the smoother amplitude decay, reduced peak responses, and more spatially balanced vibration distribution observed for the Span 3 configuration. Consequently, the trench and shear wall operate in a complementary and sequential manner, effectively reducing both direct and reflected vibration energy and thereby enhancing vibration control across all monitoring locations.

3.3. Integrated Discussion and Design Implications

The collective findings demonstrate that the spatial positioning of shear walls plays a decisive role in controlling the vibration response of reinforced-concrete buildings subjected to train-induced ground motions. The influence of wall location exhibits a clear transition from localized to global mitigation effectiveness, depending on its relative position within the structural frame.

- **Near-source placement (Span 1):** This configuration provides strong but highly localized damping performance. Although the shear wall effectively suppresses vibrations in its immediate vicinity, the abrupt stiffness discontinuity introduced into the structural system promotes secondary wave reflections and localized amplification in regions farther from the excitation source.

- **Intermediate placement (Span 2):** Positioning the wall at the mid-span results in improved redistribution of vibration energy throughout the frame, thereby reducing severe local response concentrations. Nevertheless, the attenuation pattern remains spatially nonuniform across the building width.

- **Distal placement (Span 3):** Locating the shear wall farthest from the trench produces the most uniform and globally effective vibration mitigation. In this configuration, simultaneous reductions in Peak Particle Velocity (PPV), Root Mean Square (RMS) velocity, and vibration decibel level (VdB) are achieved at all roof monitoring locations.

Among the three evaluation metrics considered, the Root Mean Square (RMS) velocity emerged as the most robust and physically representative indicator of global vibration-control performance. Unlike the instantaneous PPV measure or the logarithmically scaled VdB parameter, the RMS response reflects the cumulative vibration energy transmitted through the structure, thereby providing a more stable and comprehensive assessment of mitigation efficiency.

The results further reveal the synergistic interaction between the open trench and the optimally positioned shear wall. The trench primarily functions as a path-based isolation mechanism by scattering and filtering a substantial portion of the incident surface-wave energy before it reaches the building foundation. The shear wall, particularly in the Span 3 configuration, complements this mechanism by acting as a receiver-based damping component that absorbs, redistributes, and dissipates the residual vibrational energy throughout the superstructure.

This hybrid mitigation strategy effectively combines external wave interception with internal structural energy dissipation, leading to smoother amplitude decay, reduced resonance susceptibility, and improved overall vibration attenuation.

From a practical design standpoint, the present study establishes a comprehensive framework for the development of vibration-resilient structural systems in railway-adjacent environments. The integration of passive trench barriers with strategically positioned shear walls enables substantial improvements in vibration mitigation without significant increases in construction complexity or material consumption. Consequently, such an approach offers considerable potential for enhancing structural performance, serviceability, and occupant comfort, while also supporting the development of sustainable and vibration-sensitive urban infrastructure.

4. Conclusion

This study presents a comprehensive numerical investigation into the coupled influence of shear wall placement and a 3 m-deep open trench on the vertical vibration response of a six-story reinforced-concrete (RC) building subjected to train-induced ground excitation. The analyses were performed using a rigorously validated finite-element framework incorporating full soil–structure–trench interaction, thereby enabling a realistic representation of wave propagation from the railway track through the soil medium to the building foundation and superstructure. Four structural configurations were examined: a reference model without a shear wall and three braced models in which the wall was positioned in the first, second, and third spans of the structural frame. In all cases, a 3 m-deep open trench located between the railway embankment and the building was included to evaluate the coupled mitigation mechanism.

The numerical results demonstrate that the location of the shear wall exerts a dominant influence on vibration amplitude, spatial distribution, and energy dissipation characteristics. Placement of the wall in the first span, directly adjacent to the trench, produced strong localized damping at the point closest to the wall; however, it also generated amplified responses at more distant locations due to stiffness discontinuities and internal wave reflections within the frame. The second-span configuration produced a comparatively more balanced response, although attenuation remained spatially nonuniform. In contrast, the third-span arrangement, in which the wall was located farthest from the excitation source, provided the most effective and spatially consistent vibration reduction, characterized by smoother attenuation and lower response amplitudes across all monitoring points.

Quantitative evaluation using Peak Particle Velocity (PPV), Root Mean Square (RMS) velocity, and vibration decibel level (VdB) confirmed these observations. Among these parameters, the RMS velocity proved to be the most representative indicator of global vibration behavior, as it reflects the cumulative energy transmitted through the structural system rather than isolated peak responses. Relative to the unbraced configuration, the optimal third-span arrangement achieved reductions of approximately 30% in PPV, 10–15% in RMS velocity, and 2–3% in VdB, demonstrating its superior vibration mitigation performance and improved serviceability characteristics.

The underlying mechanism responsible for this behavior can be attributed to the synergistic interaction between the open trench and the shear wall. The trench functions primarily as a path-based isolation barrier, scattering and attenuating a substantial portion of the incoming wave field before it reaches the building. The shear wall then acts as a receiver-based structural damping component that redistributes and dissipates the remaining vibration energy within the superstructure. When spatially separated, as in the third-span configuration, this sequential mitigation process promotes smoother amplitude decay and reduces internal resonance effects within the building.

The principal conclusions of the present study can therefore be summarized as follows:

- The spatial location of the shear wall significantly influences vibration mitigation performance, reflecting the coupled interaction between the trench and the structural stiffening mechanism. In particular, positioning the shear wall farther from the excitation source (Span 3) results in the most stable, uniform, and effective reduction in structural vibration response, indicating that the combined action of wave attenuation by the trench and stiffness redistribution by the shear wall governs the overall mitigation efficiency.

- The RMS velocity represents the most robust and physically meaningful vibration metric, as it captures the cumulative energy transmission and dissipation within the structural system.

- The combined trench–wall mitigation mechanism demonstrates that distributed stiffness and sequential energy absorption are more effective than localized structural stiffening in achieving sustainable vibration control.

Overall, the findings establish a practical hybrid mitigation strategy that integrates passive ground isolation through an open trench with strategically positioned structural stiffening via shear walls. This approach provides a viable framework for the design of vibration-resilient buildings located near railway corridors, offering engineers a systematic basis for improving structural performance and occupant comfort under train-induced dynamic loading. Future research should consider nonlinear soil behavior, frequency-dependent train loading spectra, and multiple trench configurations to further extend and generalize the proposed vibration mitigation strategy.

References

Adam, M., Pflanz, G., and Schmid, G. (2000). Two- and three-dimensional modelling of half-space and train-track embankment under dynamic loading. *Soil Dynamics and Earthquake Engineering*, 19(8):559–573.

Adam, M. and von Estorff, O. (2005). Reduction of train-induced building vibrations by using open and filled trenches. *Computers & Structures*, 83(1):11–24.

Beskos, D., Dasgupta, B., and Vardoulakis, I. (1986). Vibration isolation using open or filled trenches - part 1 : 2-d homogeneous soil. *Computational Mechanics*, 1:43–63.

Buonsanti, M., Cirianni, F., Leonardi, G., Adolfo, S., and Francesco, S. (2009). Mitigation of railway traffic induced vibrations: The influence of barriers in elastic half-space. *Advances in Acoustics and Vibration*.

Colaço, A., Liravi, H., Soares, P., Ninic, J., and Costa, P. (2025). Ground-borne vibrations induced by railway traffic: Impact, prediction, mitigation and future perspectives. *Vibration*, 8.

Connolly, D., Marecki, G., Kouroussis, G., Thalassinakis, I., and Woodward, P. (2016). The growth of railway ground vibration problems - a review. *Science of The Total Environment*, 568:1276–1282.

Farsiani, M. and Shodja, H. M. (2026). An augmented surface impedance theory for acoustically actuated magneto-electro-elastic nanospheres with terahertz nanoantenna applications. *Mechanics of Materials*, 212:105515.

Farsiani, M., Shodja, H. M., and Behzadan, A. (2024). Mathematical analysis of an acoustically actuated nanospherical antenna with terahertz frequency range applications in the framework of generalized spectral magneto-electro-elastodynamic interface theory. *Phys. Rev. B*, 109:094109.

Grębowski, K. and Zielińska, M. (2026). Finite element modelling of dynamic interactions caused by high-speed train passage on historic railway bridge. *Structures*, 88:111898.

He, Y., Liu, B., and Zhang, H. (2025). Study on the effect of subway construction on adjacent architectural heritages and protection measures. *Scientific Reports*, 15.

Hung, H. H., Yang, Y., and Chang, D. (2004). Wave barriers for reduction of train-induced vibrations in soils. *Journal of Geotechnical and Geoenvironmental Engineering - J GEOTECH GEOENVIRON ENG*, 130.

Jesmani, M., Fallahi, A., and Kashani, H. (2012). Effects of geometrical properties of rectangular trenches intended for passive isolation in sandy soils. *Earth Science Research*, 1:137–151.

Jones, C. and Block, J. (1996). Prediction of ground vibration from freight trains. *Journal of Sound and Vibration*, 193(1):205–213.

Kattis, S., Polyzos, D., and Beskos, D. (1999). Modelling of pile wave barriers by effective trenches and their screening effectiveness. *Soil Dynamics and Earthquake Engineering*, 18(1):1–10.

Kontoni, D.-P. and Farghaly, A. (2020). Mitigation of train-induced vibrations on nearby high-rise buildings by open or geofoam-filled trenches. *Journal of Vibroengineering*, 22:416–426.

Kouroussis, G., Connolly, D., and Verlinden, O. (2014). Railway induced ground vibrations—a review of vehicle effects. *International Journal of Rail Transportation*, 2:69–110.

Leung, K., Vardoulakis, I., Beskos, D., and Tassoulas, J. (1991). Vibration isolation by trenches in continuously nonhomogeneous soil by the bem. *Soil Dynamics and Earthquake Engineering*, 10(3):172–179.

Li, T., Su, Q., and Kaewunruen, S. (2019). Saturated ground vibration analysis based on a three-dimensional coupled train-track-soil interaction model. *Applied Sciences*, 9:4991.

Mansur, W. and Brebbia, C. (1982). Formulation of the boundary element method for transient problems governed by the scalar wave equation. *Applied Mathematical Modelling*, 6(4):307–311.

Mino, G., Giunta, M., and Liberto, C. (2009). Assessing the open trenches in screening railway ground-borne vibrations by means of artificial neural network. *Advances in Acoustics and Vibration*, 2009.

Mylonakis, G. (2000). Seismic soil-structure interaction: Beneficial or detrimental? *Journal of Earthquake Engineering - J EARTHQU ENG*, 4:277–301.

Oner, M. and Dong, S. B. (1988). Analysis of in-plane waves in layered half-space by global-local finite element method. *Soil Dynamics and Earthquake Engineering*, 7(1):2–8.

Peplow, A., Jones, C., and Petyt, M. (1999). Surface vibration propagation over a layered elastic half-space with an inclusion. *Applied Acoustics*, 56(4):283–296.

Remennikov, A. and Kaewunruen, S. (2008). A review of loading conditions for railway track structures due to train and track vertical interaction. *Structural Control and Health Monitoring*, 15:207 – 234.

Sadeghi, J., Valipouri, Z., and Esmaeili, M. (2025). Evaluation of shear walls effect in mitigating metro-induced vibrations in adjacent buildings. *Structures*, 82:110503.

Shodja, H. M., Farsiani, M., and Behzadan, A. (2023). Tensor spherical harmonics analysis of electro-elastostatic fields in a spherically isotropic multiphase functionally graded piezoelectric medium. *Proceedings of the Royal Society A: Mathematical, Physical and Engineering Sciences*, 479(2276):20230267.

Zakeri, J., Esmaeili, M., and Mosayebi, S. A. (2014). Numerical investigation of the effectiveness of a step-shaped trench in reducing train-induced vibrations. *Proceedings of the Institution of Mechanical Engineers, Part F: Journal of Rail and Rapid Transit*, 228:298–306.

Zhai, W., Han, Z., Chen, Z., Ling, L., and Zhu, S. (2019). Train-track-bridge dynamic interaction: a state-of-the-art review. *Vehicle System Dynamics*, 57.

Zhao, S., Lu, C., Shen, J., and Zhao, M. (2025). Train-induced vibration analysis and isolation trench measures in metro depot structures. *Applied Sciences*, 15:4219.